

# Simulation of Contrast Agent Enhanced Ultrasound Imaging based on Field II

Tobias Gehrke, Heinrich M. Overhoff

Medical Engineering Laboratory, University of Applied Sciences Gelsenkirchen  
tobias.gehrke@fh-gelsenkirchen.de

**Abstract.** Pulse-echo ultrasound signal formation can be simulated by numerical emulation of the process chain: emit signal – electromechanical emit transformation – wave propagation and scattering – electromechanical receive transformation – receive signal. The simulation software Field II is intended for simulation of linear ultrasound systems. We present an extension to Field II that enables the inclusion of nonlinear oscillations of ultrasound contrast agent bubbles into the simulation. An example is given for contrast agent enhanced imaging of a virtual vessel phantom probed by a linear array transducer.

## 1 Introduction

Ultrasound contrast agents consist of gas-filled microbubbles whose radii oscillate when exposed to sonic waves emitted from an ultrasound transducer. Simulation enables evaluation of novel contrast imaging modalities with respect to different transducer geometries, electronic settings and irradiated phantoms as well as various concentrations and types of contrast agent, without costly experiments.

The software package Field II [1] has become a standard tool in the simulation of ultrasonic pulse echo imaging. This software is limited to the simulation of linear passive scattering from tissue inhomogeneities. However, the physics of bubble dynamics is nonlinear and can therefore not be modelled within the Field II framework. Approaches to overcome this limitation have been undertaken, but are either limited to linear bubble oscillation [2] or rely on empirical data that has to be acquired prior to the simulation [3]. We present an extension to Field II that enables inclusion of signals originating from nonlinear contrast agent bubble oscillations. Our approach is entirely derived from basic physical relations what makes empirical modification dispensable.

## 2 Materials and Methods

### 2.1 Basic Physical Relations

The process of contrast agent enhanced medical ultrasound imaging is determined by the physical relations in three coupled physical domains: The ultrasound transducer, the propagation medium, i. e. the human body, and the gas phase inside the contrast agent bubbles.

**Electromechanical Transducer Behaviour** Assuming linearity, an ultrasound transducer can be characterized by a four pole model that relates the force  $F(\omega)$  onto and the velocity  $\bar{V}(\omega)$  of the transducer's front face  $\mathcal{S}_t$ , to voltage  $E(\omega)$  and current  $I(\omega)$  at its electrodes [4]. For a fix electrical impedance and a time invariant radiation impedance, it can be reduced to a two pole model. Making a distinction between transmission and reception for convenience it reads

$$\bar{V}(\omega) = H_{\text{trm}}(\omega)E_{\text{exc}}(\omega) \Rightarrow \bar{v}(t) = h_{\text{trm}}(t) * e_{\text{exc}}(t) \quad (1)$$

$$E_{\text{rec}}(\omega) = H_{\text{rec}}(\omega)F(\omega) \Rightarrow e_{\text{rec}}(t) = h_{\text{rec}}(t) * f(t), \quad (2)$$

with  $*$  denoting convolution <sup>1</sup>. Voltage and force are coupled by the electromechanical transfer functions  $H_{\text{trm}}(\omega)$  and  $H_{\text{rec}}(\omega)$  for transmission and reception respectively in frequency domain or the corresponding impulse responses  $h_{\text{trm}}(t)$  and  $h_{\text{rec}}(t)$  in time domain.

**Wave Propagation** Under linear conditions, propagation of pressure waves  $p(\mathbf{r}, t)$  inside a medium with density  $\rho(\mathbf{r})$  and compressibility  $\kappa(\mathbf{r})$  is described by [5]

$$\nabla (\rho(\mathbf{r})^{-1} \nabla p(\mathbf{r}, t)) - \kappa(\mathbf{r}) \ddot{p}(\mathbf{r}, t) = 0 \quad (3)$$

For a homogeneous medium with density  $\bar{\rho}$ , compressibility  $\bar{\kappa}$ , and speed of sound  $\bar{c} = (\bar{\rho}\bar{\kappa})^{-\frac{1}{2}}$  wave equation (3) reduces to

$$\nabla^2 p(\mathbf{r}, t) - \bar{c}^{-2} \ddot{p}(\mathbf{r}, t) = 0 \quad (4)$$

**Bubble Dynamics** Under equilibrium conditions  $p(\mathbf{r}, t) = p_0$ , the radius of a single spherical gas-bubble immersed in an incompressible homogeneous fluid is  $R(t) = R_0$ . The bubble dynamics is modelled by the Rayleigh-Plesset equation

$$\bar{\rho} \left( R(t) \ddot{R}(t) + \frac{3}{2} \dot{R}(t)^2 \right) = \left( p_0 + \frac{2\sigma}{R_0} - p_v \right) \left( \frac{R_0}{R(t)} \right)^{3\gamma} - \frac{2\sigma + 4\eta \dot{R}(t)}{R(t)} + p_v - p(\mathbf{r}, t) \quad (5)$$

which relates a varying pressure  $p(\mathbf{r}, t)$  to oscillation of  $R(t)$  [4]. Besides its density  $\bar{\rho}$ , the surrounding liquid is characterized by its dynamic viscosity  $\eta$  and vapour pressure  $p_v$ . The quantity  $\sigma$  is the surface tension of the liquid-gas interface, and  $\gamma$  denotes the polytropic exponent of the gas inside the bubble.

## 2.2 System Model

To model the process of pulse-echo signal formation, the pressure field  $p(\mathbf{r}, t)$  is decomposed into three different fields: The incident pressure  $p_i(\mathbf{r}, t)$  would be present in a homogeneous i. e. scatterer and bubble free medium due to radiation from the transducer, the fields  $p_s(\mathbf{r}, t)$  and  $p_b(\mathbf{r}, t)$  are the additional pressures from passive scattering and active bubble emission.

<sup>1</sup> The function arguments  $t$  on the right hand side indicate that two functions of time are convolved. This notation shall not imply that the convolution at time  $t$  is computed solely from the function values at time  $t$ .

**Incident Pressure Field** The incident pressure  $p_i(\mathbf{r}, t)$  originating from a transducer at position  $\mathbf{r}_t$  is calculated by a Green's function solution to the homogeneous wave equation (4). If the transducer is assumed to be placed in an infinite rigid baffle  $\mathcal{S}_b$ , the boundary conditions are

$$\frac{\partial}{\partial \mathbf{n}} p_i(\mathbf{r}, t) \Big|_{\mathbf{r}=\mathbf{r}_t+\mathbf{s}} = \begin{cases} -\bar{\rho} w(\mathbf{s}) \frac{\partial \bar{v}(t)}{\partial t}, & (\mathbf{r}_t + \mathbf{s}) \in \mathcal{S}_t \\ 0, & (\mathbf{r}_t + \mathbf{s}) \in (\mathcal{S} \setminus \mathcal{S}_t) \end{cases} \quad (6)$$

Here  $\mathbf{n}$  denotes the normal vector onto transducer surface  $\mathcal{S}_t$  and  $\mathbf{s}$  points towards any position on the transducer surface or baffle. Position dependency of the transducer displacement is accounted for by the surface velocity distribution function  $w(\mathbf{s})$ . The Green's function solution to this problem is [6]

$$p_i(\mathbf{r}, t) = \iint_{\mathcal{S}_t} \int_0^t 2w(\mathbf{s}) \frac{\partial \bar{v}(\tau)}{\partial \tau} \frac{\delta(t - \tau - |\mathbf{r} - (\mathbf{r}_t + \mathbf{s})|/\bar{c})}{4\pi|\mathbf{r} - (\mathbf{r}_t + \mathbf{s})|} d\tau d\mathbf{s} \quad (7)$$

By defining a spatial impulse response

$$h_{\text{spt}}(\mathbf{r}, t) = \iint_{\mathcal{S}_t} w(\mathbf{s}) \frac{\delta(t - \tau - |\mathbf{r} - (\mathbf{r}_t + \mathbf{s})|/\bar{c})}{4\pi|\mathbf{r} - (\mathbf{r}_t + \mathbf{s})|} d\mathbf{s} \quad (8)$$

and using the electromechanical relation (1), the incident pressure is given by

$$p_i(\mathbf{r}, t) = 2\bar{\rho}e(t) * h_{\text{trm}}(t) * \frac{\partial}{\partial t} h_{\text{spt}}(\mathbf{r}, t) \quad (9)$$

**Scattered Pressure Field** The left hand side of the homogeneous wave equation (4) is subtracted on both sides of its inhomogeneous counterpart (3) to derive the component of the pressure field due to an inhomogeneity  $q$  [7]:

$$\begin{aligned} \nabla^2 p_{\text{sq}}(\mathbf{r}, t) - \bar{c}^{-2} \ddot{p}_{\text{sq}}(\mathbf{r}, t) &= \bar{c}^{-2} \left( \frac{\kappa(\mathbf{r})}{\bar{\kappa}} - 1 \right) \ddot{p}(\mathbf{r}, t) - \nabla \left[ \left( \frac{\bar{\rho}}{\rho(\mathbf{r})} - 1 \right) \nabla p(\mathbf{r}, t) \right] \\ &\approx V_q \bar{c}^{-2} \left[ \left( \frac{\kappa(\mathbf{r}_q)}{\bar{\kappa}} - 1 \right) + \left( \frac{\bar{\rho}}{\rho(\mathbf{r}_q)} - 1 \right) \cos \Theta_q \right] \ddot{p}(\mathbf{r}_q, t) \end{aligned} \quad (10)$$

Comparison with (4) shows that the scatter act as a source to the homogeneous wave equation. The approximation has been made by lumping the scatterer with volume  $V_q$  and irradiation angle  $\Theta_q$  into a single point at  $\mathbf{r}_q$  [7] and using the paraxial approximation [6, 8]. This is tolerable if the scatterer is small and sufficiently far away from the transducer.

**Bubble Emitted Pressure Field** Equivalently to the scatterers, the bubbles are modelled as point sources that radiate into a homogeneous medium:

$$\nabla^2 p_{\text{bq}}(\mathbf{r}, t) - \bar{c}^{-2} \ddot{p}_{\text{bq}}(\mathbf{r}, t) = \left( p_0 + \frac{2\sigma_q}{R_{0q}} - p_v \right) \left( \frac{R_{0q}}{R_q(t)} \right)^{3\gamma} - \left( p_0 + \frac{2\sigma_q}{R_q(t)} - p_v \right) \quad (11)$$

The right hand side source term is the pressure just beyond the wall of a gas-bubble  $q$  [4]. The time varying bubble radius  $R_q(t)$  depends on the pressure  $p(\mathbf{r}_q, t)$  and can be obtained from the Rayleigh-Plesset equation (5).

**Total Pressure Field** The incident field in a pulse echo system is travelling outwards and does hence not contribute to the force onto the receiving transducer. The total echo field from all  $Q$  scatterers and bubbles is thus obtained by the Green's function solution to (10) and (11) respectively [6, 7]:

$$p(\mathbf{r}, t) = \sum_{q=1}^Q \int_0^t \mathfrak{R}_q \{ p(\mathbf{r}_q, \tau) \} \frac{\delta(t - \tau - |\mathbf{r} - \mathbf{r}_q|/\bar{c})}{4\pi|\mathbf{r} - \mathbf{r}_q|} d\tau \quad (12)$$

The operator  $\mathfrak{R}_q \{ \cdot \}$  acting onto pressure  $p(\mathbf{r}, t)$  denotes the source terms, i. e. right hand sides in (10) or (11). If the fields  $p_s(\mathbf{r}, t)$  and  $p_b(\mathbf{r}, t)$  are weak compared to the incident field  $p_i(\mathbf{r}, t)$ , the latter can replace the total pressure field  $p(\mathbf{r}, t)$  on the right hand side of (12), what is known as Born approximation [6].

**Force onto Receiver** An ultrasound transducer is sensitive to the force

$$\begin{aligned} f(t) &= \iint_{\mathcal{S}_t} w(\mathbf{s}) p(\mathbf{r}_t + \mathbf{s}, t) d\mathbf{s} \\ &= \iint_{\mathcal{S}_t} w(\mathbf{s}) \sum_{q=1}^Q \int_0^t \mathfrak{R}_q \{ p_i(\mathbf{r}_q, \tau) \} \frac{\delta(t - \tau - |\mathbf{r}_t + \mathbf{s} - \mathbf{r}_q|/\bar{c})}{4\pi|\mathbf{r}_t + \mathbf{s} - \mathbf{r}_q|} d\tau d\mathbf{s} \quad (13) \end{aligned}$$

that acts onto its surface  $\mathcal{S}_t$ . The spatial dependency of the transducer's receive sensitivity is equal to the surface velocity distribution  $w(\mathbf{s})$  in transmit mode [8]. The spatial impulse response (8) can be used to denote (14) in a short way:

$$f(t) = \sum_{q=1}^Q \mathfrak{R}_q \{ p_i(\mathbf{r}, t) \} * h_{\text{spt}}(\mathbf{r}_q, t) \quad (14)$$

**Receive Signal** The electromechanical receive dynamics (2) and the models of the subsystems (9), and (14) can be connected to an overall system model:

$$e_{\text{rec}}(t) = \sum_{q=1}^Q \mathfrak{R}_q \{ 2\bar{\rho}e_{\text{exc}}(t) * h_{\text{trm}}(t) * \frac{\partial}{\partial t} h_{\text{spt}}(\mathbf{r}_q, t) \} * h_{\text{spt}}(\mathbf{r}_q, t) * h_{\text{rec}}(t) \quad (15)$$

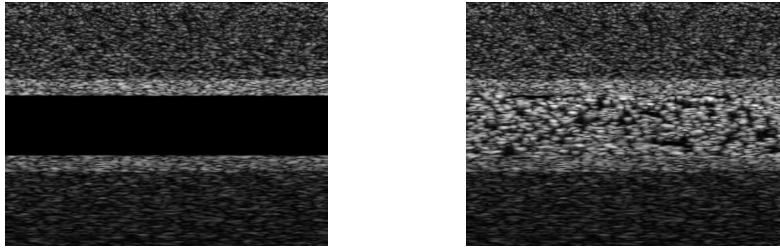
### 2.3 Implementation

A program that computes the signal processing chain from the exciting voltage  $e_{\text{exc}}(t)$  to the receive voltage trace  $e_{\text{rec}}(t)$ , as described by (15), has been developed in Matlab (The Mathworks Inc., Natick, MA, USA).

For most transducers, analytic solutions for the spatial impulse responses are unknown. To compute (8) Field II, which provides a powerful numerical method to calculate impulse responses for numerous transducer geometries [1], is used.

The program solves the Rayleigh-Plesset equation (5) numerically by a variable order method for every combination of bubbles and aperture elements. To increase the simulation speed, a critical level for the incident pressure has been introduced below which computation of the bubble oscillation is omitted.

**Fig. 1.** Simulated B-mode images without (left) and with contrast agent (right)



### 3 Results

To test the simulation program, an ultrasound machine with a 256-element linear array and 3.5 MHz centre frequency has been emulated. In Fig. 1 simulated B-mode images of a blood vessel with 15 mm diameter are shown without and with contrast agent enhancement. The virtual phantom consists of 30 000 randomly distributed scatterers that mimic the vessel walls and surrounding muscular tissue and 1000 air-filled bubbles with normally distributed radii (mean  $\bar{R}_0 = 1 \mu m$ , standard deviation  $s_{R_0} = 0.3 \mu m$ ) as contrast agent.

### 4 Discussion

Combination of a numerical solver for the Rayleigh-Plesset equation with Field II can consistently simulate contrast agent enhanced ultrasound imaging. The program is useful for the development of novel contrast agent imaging methods.

### References

1. Jensen JA. Field: A program for simulating ultrasound systems. In: Proceedings of the 10th Nordic-Baltic Conference on Biomedical Imaging; 1996. p. 351–3.
2. Gerfault L, Cachard C, Gimenez G. Simulation of echographic image of contrast agent. In: IEEE Ultrasonics Symposium; 1998. p. 1815–8.
3. Durning B, Laval J, Rognin N, et al. Ultrasound signals and images simulation of phantoms with contrast agent. In: IEEE International Ultrason Ferroelectr Freq Control Joint 50th Anniversary Conference; 2004. p. 1710–3.
4. Szabo TL. Diagnostic Ultrasound Imaging. Amsterdam: Elsevier; 2004.
5. Insana MF, Brown DG. Acoustic scattering theory applied to soft biological tissues. In: Shung KK, Thieme GA, editors. Ultrasonic scattering in biological tissues. Boca Raton: CRC Press; 2000. p. 75–124.
6. Jensen JA. A model for the propagation and scattering of ultrasound in tissue. IEEE Trans Ultrason Ferroelectr Freq Control. 1991;89(1):182–90.
7. Gehrke T, Cheikhrouhou F, Overhoff HM. A simulation program for ultrasound tomography imaging based on Field II. Proc IFMBE. 2005;11:4393–8.
8. Lhémy A. Impulse-response method to predict echo-responses from targets of complex geometry. Part I: Theory. J Acoust Soc Am. 1991;90(5):2799–807.